Journal of Applied Mathematics and Physics, 2013, 1, 6-11
http://dx.doi.org/10.4236/jamp.2013.14002 Published Online October 2013 (http://www.scirp.org/journal/jamp)

Parallel Simulation of 3D Wave Propagation by Domain Decomposition

Galina Reshetova[1], Vladimir Tcheverda[2], Dmitry Vishnevsky[2]
[1]The Institute of Computational Mathematics and Mathematical Geophysics, Siberian Branch of the RAS, Russia
[2]The Institute of Petroleum Geology and Geophysics, Siberian Branch of the RAS, Russia
Email: kgv@nmsf.sscc.ru

Received July 2013

ABSTRACT

In order to perform large scale numerical simulation of wave propagation in 3D heterogeneous multiscale viscoelastic media, Finite Difference technique and its parallel implementation based on domain decomposition is used. A couple of typical statements of borehole geophysics are dealt with—sonic log and cross well measurements. Both of them are essentially multiscales, which claims to take into account heterogeneities of very different sizes in order to provide reliable results of simulations. Locally refined spatial grids help us to avoid the use of redundantly tiny grid cells in a target area, but cause some troubles with uniform load of Processor Units involved in computations. We present results of scalability tests together with results of numerical simulations for both statements performed for some realistic models.

Keywords: Seismic Wave propagation; Sonic Log; Numerical Simulation; Domain Decomposition

1. Introduction

The most effective way to improve resolving ability of any wave images is to increase dominant frequency of a sounding pulse. But Earth media attenuate and disperse propagating waves. Both these effects are often quantified by the Quality Factor Q. This factor describes relative dissipation of seismic energy per unit volume per unit cycle. If attenuation is not too strong, Quality Factor can be treated as a number of wavelengths a wave can propagate through a medium before its amplitude was decreased in e^{π} times.

Both fields and laboratory experiments prove that this parameter can be treated as independent on time frequency for rather wide frequency range [5]. Therefore the higher is the dominant frequency of a source pulse, the shorter is the distance with reliable level of signal-to-noise ratio. So, in order to get an image with high resolution it is necessary to place acquisition system as close to the target object as possible. The only way to do this is to place sources and/or receivers within boreholes drilled in the vicinity of the target object. In its own turn presence of a well filled with a drilling mud brings essential peculiarities to wave fields and should be taken into account in model description. In its own turn, this claims use of locally refined grids in order to catch heterogeneities of the smallest scale only.

The paper deals with numerical simulation of waves propagation within viscoelastic media for the following borehole based geophysical methods:

a) **Sonic Log**—sources and receivers are within the same borehole and the main task is monitoring of casing pipe integrity and recovery of near well-bore vicinity. Multiscale nature of the problem becomes apparent in the presence of heterogeneities of at least two different scales-distance source/receiver and borehole radius. If one deals with a cased borehole there is third scale-structure of the casing. Fourth scale can be introduced by a medium;

b) **Cross-well Tomography**—sources and receivers are placed within adjacent boreholes encircling a target object. This problem possesses two extremely different scales-borehole diameter and distance between sources and receivers.

2. Viscoelastic Media

Any process of wave propagation within linear elastic medium is governed by two groups of equations:

1) Motion equations (Newton's law);

2) State equation that connects stress and strain tensors (Hook's law).

In reality rocks possess intrinsic attenuation produced by their "memory": stress state at some instant t is determined by the "history" of strains. We will suppose that all processes are causal, that is the current state of the medium does not depend on the future by no means. So, in the most general form the Hook's law for these mate-

rials can be written down in the following way:

$$\sigma_{ij}(x,t) = G_{ijkl}(x,0)\varepsilon_{kl}(x,t) + \int_0^t G_{ijkl}(x,\tau)\frac{\partial \varepsilon_{kl}(x,t-\tau)}{\partial \tau}d\tau$$

For isotropic viscoelastic materials relaxation tensor simplifies to the following one:

$$G_{ijkl} = \delta_{ij}\delta_{kl}\Lambda(x,t) + 2\delta_{ik}\delta_{jl}M(x,t)$$

Numerical resolution of integro-differential equations (1) is very troublesome. The most convenient way is to represent state equation in a differential form on a base of mechanical analog of a viscoelastic material like a set of rings and plungers known as Generalized Linear Standard Solid (see [2]). Moreover, real data, both field and laboratory, proved that (see [5-7]): *A correct modeling scheme should yield a constant Quality Factor Q and the corresponding dispersion relation.*

The common way to implement these properties of real media in mathematical model is again just mentioned **Generalized Standard Linear Solid** (GSLS). For this model the Hook's law is written down as:

$$\sigma = \sum_{j=1}^{L}\sigma_j;$$

$$\sigma_i + \tau_{\sigma i}\frac{\partial \sigma_i}{\partial t} = M_R\left(\varepsilon + \tau_{\varepsilon i}\frac{\partial \varepsilon}{\partial t}\right)$$

and introduces Quality Factor as:

$$Q(\omega) = \frac{1 - L + \sum_{l=1}^{L}\frac{1+\omega^2\tau_{\sigma l}\tau_{\varepsilon l}}{1+\omega^2\tau_{\sigma l}^2}}{\sum_{l=1}^{L}\frac{\omega(\tau_{\varepsilon l}-\tau_{\sigma l})}{1+\omega^2\tau_{\sigma l}^2}}$$

The problem is how to choose a set of parameters $\tau_{\sigma i}, \tau_{\varepsilon i}$ providing desired behavior of Quality Factor over a predefined interval of time frequencies.

We resolve it on the base of Least Squares techniques:

$$J(\tau_\sigma, \tau_\varepsilon) = \int_{\omega_1}^{\omega_2} |Q^{-1}(\omega) - Q^{-1}|^2 \, d\omega \to \min$$

In order to find desired sets of relaxation times we applied τ-method proposed in [1] and modified recently in [3]. Its main advantage is essential reduction of a number of relaxation times-for realistic values of Quality Factor ($Q > 10$) one can manage with single value of τ_ε (and keep it the same through the target area!) and a couple of τ_σ. Application of τ-method for GSLS gives the following representation of Hook's law:

$$\sigma(t,x) = M_R(1+L\tau)\varepsilon(t,x) - \tau - M_R\sum_{l=1}^{L}\frac{1}{\tau_{\sigma l}}\int_0^t e^{-\frac{t-\tau}{\tau_{\sigma l}}}\varepsilon(\tau,x)d\tau$$

Let us differentiate this relation with respect to time t:

$$\frac{\partial \sigma}{\partial t} = M_R(1+L\tau)\frac{\partial \varepsilon(t,x)}{\partial t} - \tau M_R \times \sum_{l=1}^{L}\frac{1}{\tau_{\sigma l}}\left[\varepsilon(t,x) - \frac{1}{\tau_{\sigma l}}\int_0^t e^{-\frac{t-\tau}{\tau_{\sigma l}}}\varepsilon(\tau,x)\right]d\tau$$

and introduce l-th memory variable

$$r_l(t,x) = -\frac{\tau}{\tau_{\sigma l}}M_R\left[\varepsilon(t,x) - \frac{1}{\tau_{\sigma l}}\int_0^t e^{-\frac{t-\tau}{\tau_{\sigma l}}}\varepsilon(\tau,x)\right] \quad (2)$$

Straightforward differentiation of (2) provides the following equation for this variable:

$$\frac{\partial r_l}{\partial t} = -\frac{\tau}{\tau_{\sigma l}}M_R\frac{\partial v}{\partial x} - \frac{r_l(t,x)}{\tau_{\sigma l}}$$

and we come to the following system of first-order PDE for viscoelastic wave propagation:

$$\varrho\frac{\partial v}{\partial t} = \frac{\partial \sigma}{\partial x}$$

$$\frac{\partial \sigma}{\partial t} = M_R(1+L\tau)\frac{\partial v}{\partial x} + \sum_{l=1}^{L} r_l$$

$$\frac{\partial r_l}{\partial t} = -\frac{1}{\tau_{\sigma l}}\left(M_R\frac{\partial v}{\partial x} + r_l\right)$$

As one can see, implementation of GSLS claims extra independent "memory" variables per relaxation mechanism per stress component. In particular, for 3D models L mechanisms claim $6L$ new variables besides three displacements and six stresses. This leads to significant increase of memory demands for simulation of waves' propagation.

3. Parallel Implementation

Parallel Implementation is based on representation of the area of computations as superposition of disjoints subdomains touching one another along some contact surface. Each of them is assigned to specific Processor Unit (PU). Waves traveling in the model pass through different subdomains, which require communication between neighboring processors. Essentially different geometry of the target area used in Sonic Log and Cross-hole Tomography claims necessity of different approaches to Domain Decomposition (DD) as well. Let us consider both of them.

3.1. Sonic Log

Target area for this statement is a circular cylinder around the well with essential prevalence of its length in comparison with width-typical length is about 10/12 meters, while radius of this target area is no more than 1/15

meters. Taking this into account we slice the total 3D model into a number of disc-like subdomains Ω_i. Finite difference scheme assumes communication between neighboring processors requiring them to exchange function values on the interfaces between elementary discs.

It should be noted that DD on the base of this rather simple geometry easily provides possibility to guarantee uniform load of Processor Units involved in computations. Another advantage of the chosen DD is in extremely small portions of data PU should interchange at each time step and, so, extremely small waiting period before computation on the next time step would be done. The MPI (Message Passing Interface) library is applied for arranging the above-mentioned send/receive procedures and special efforts are paid in order to minimize idle time of Processor Units due to the data exchange. In order to provide this we start computations for each subdomain from its interior widening them towards interfaces and use non-blocking functions **Isend** and **Ireceive** in order to arrange data exchange between neighboring PU.

Special attention was paid to analysis of effectiveness and scalability of this approach. This analysis was performed by the series of numerical experiments performed on the cluster HKC-160 (Siberian Supercomputer Center, Novosibirsk) made of 80 computation modules (hp Integrity rx1620 with two PU Intel Itanium 2, each of 1.6 Ghz, 3 Mb cache, 4 Gb RAM) connected via 24-port commutator InfiniBand (10 Gbot, Cluster Interconnect). Peak performance of the cluster is about 1 Tflop/s.

In order to estimate *effectiveness* of parallelization, fixed computational area was decomposed on different quantity of subdomains, so simulation was performed for the same target area, but with increasing number n of PU. For each n*effectiveness* is found as

$$eff(n) = \frac{4 * time(4)}{n * time(n)} \tag{3}$$

where $time(n)$ is computer time expended by n PU for simulation. We start with $n = 4$ in order to provide from the very beginning the same amount of data exchange between adjacent PU. On **Figure 1(a)**) one can see effectiveness computed for two different lengths of computational area: 12 meters (circles) and 24 meters (rectangles). These results are completely predictable - the less is load of PU the less is effectiveness. It is confirmed by behavior of both curves - for target area of 24 meters the load of single PU is twice as many as for target area of 12 meters and decrease of effectiveness is not so sharp, but finally they become the same.

Now let us perform the series of numerical experiments in opposite manner-we fix size of elementary subdomains but increase their quantity proportionally to quantity of PU. This result one can see on **Figure 1(b)**)

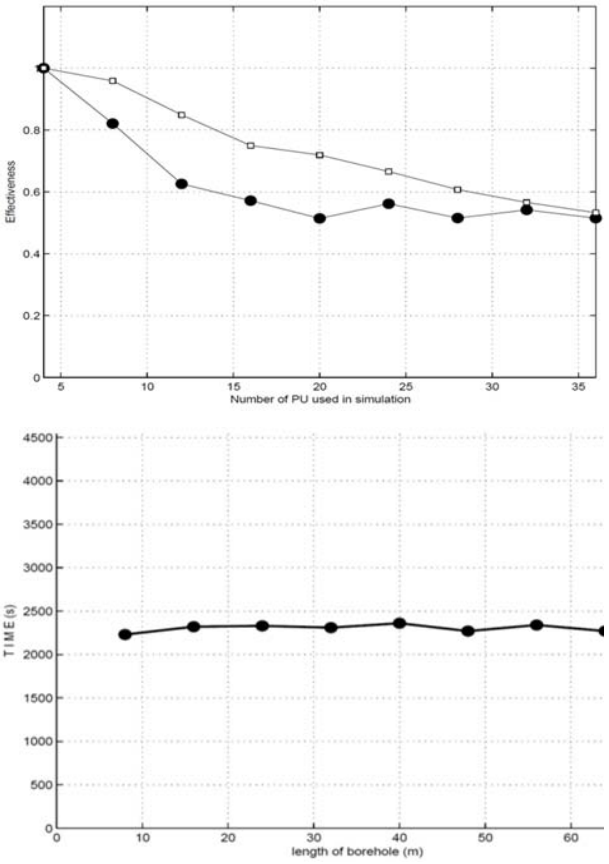

Figure 1. Scalability by numerical experimentations: Upper-Effectiveness with fixed computational area; Down-Total time with fixed load of PU.

and certain that the computational time does not change under increase of quantity of PU.

So, we can conclude, that the key parameter is ratio of amount of data being load to each of PU and amount of data it should exchange with its neighbor. The higher is this ratio the higher is effectiveness of parallelization. In particular, if this ratio is fixed it does not matter how many PU are involved in simulation.

3.2. Cross-Hole Tomography

Geometry of computational area used for cross-hole tomography is very different in comparison with previous one-now it is parallelepiped with length (distance between wells) about 300/500 meters, approximately the same depth (vertical size) and rather narrow width of $\approx$ 100 meters. Next, contrary to Sonic Log, now local grid refinement should be implemented for two different spatial locations—around wells with sources and receivers, so we need to pay special attention in order to provide uniform load of PU. The easiest way to do this is to perform straightforward application of described above 1D Domain Decomposition along cross-well direction, but it will lead to necessity of huge data exchange between PU

produced by wide contact surface between adjacent subdomains which leads to essential loss of parallelization effectiveness. In order to minimize amount of data exchanged between PU we need to reduce surface area of subdomains under fixed number of grid points per each PU—that is to choose them as close to cubes as possible. Under this approach each PU interchange data with 3/6 neighbors.

4. Numerical Experiments

To conclude the paper let us briefly consider simulation results for a couple of realistic models performed on the previously described cluster HKC-160.

Sonic Log

The series of numerical experiments have been implemented for a range of source frequencies, positions and models of surrounding elastic media. For illustration let us consider the model with well completion and vertical crack presented on the **Figures 2** and **3** and possesses the following structure:

1) Vertical borehole with radius 0.1 m filled with a mud with V_p =1500 m/s, ϱ =1000 kg/m^3, Quality Factor $Q = 65$;
2) Steel tube encircling borehole; its width is equal to 0.01 m, wave propagation velocities $V_p = 5600$ m/s, $V_s = 3270$ m/s, ϱ =7830 kg/m^3, Quality Factor $Q = 100$;
3) The casing around steel tube; its width is equal to 0.04 m, its elastic parameters are the following: V_p = 4200 m/s, V_s = 2425 m/s, ϱ = 2400 kg/m^3, Quality Factor $Q = 80$;
4) Background-homogeneous viscoelastic layer with wave propagation velocities V_p = 4989 m/s, V_s = 2605 m/s, ϱ = 2400 kg/m^3, Quality Factor $Q = 100$;
5) Background-homogeneous viscoelastic layer with wave propagation velocities V_p = 3208 m/s, V_s = 1604 m/s, ϱ = 2400 kg/m^3, Quality Factor $Q = 60$;

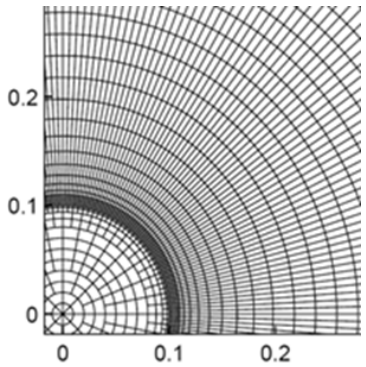

Figure 2. Radial and azimuthal grid refinement around well completion.

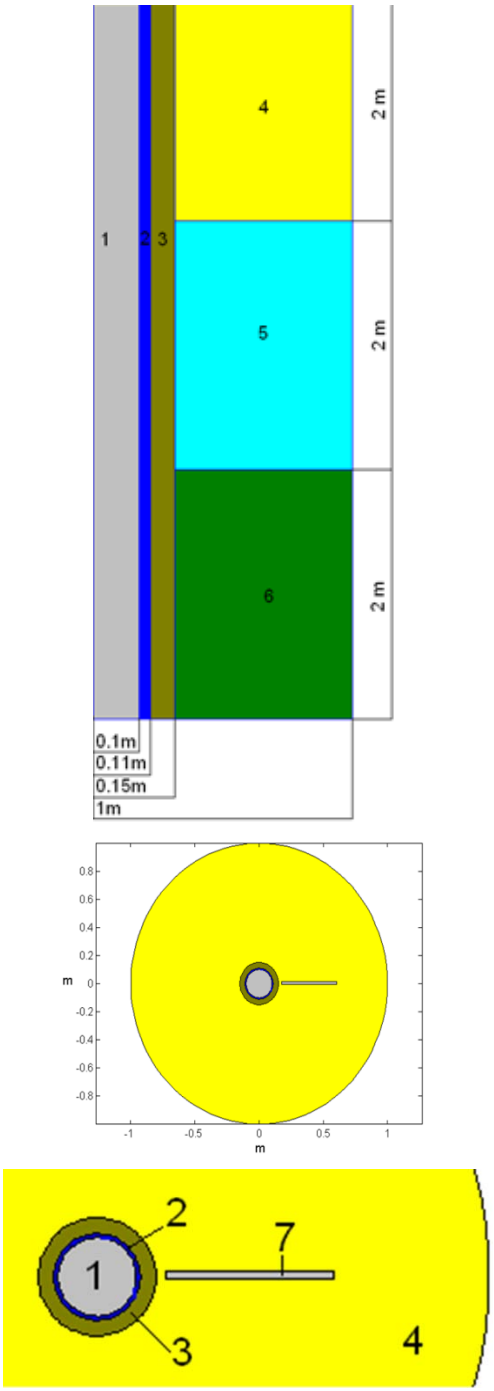

Figure 3. Upper—Vertical cross-section of the model; Middle—Horizontal cross-section of the model; Down—Zoomed version of Middle figure.

6) Background-homogeneous viscoelastic layer with wave propagation velocities V_p = 2650 m/s, V_s = 1219 m/s, ϱ = 2400 kg/m^3, Quality Factor $Q = 15$;
7) Vertical crack started at r = 0.18 m and finished at r = 0.55 m, with 0.02 m in width ((see images b) and c)) filled with the same mud as within the borehole.

On the **Figure 4** one can see snapshots stress σ_{rr}

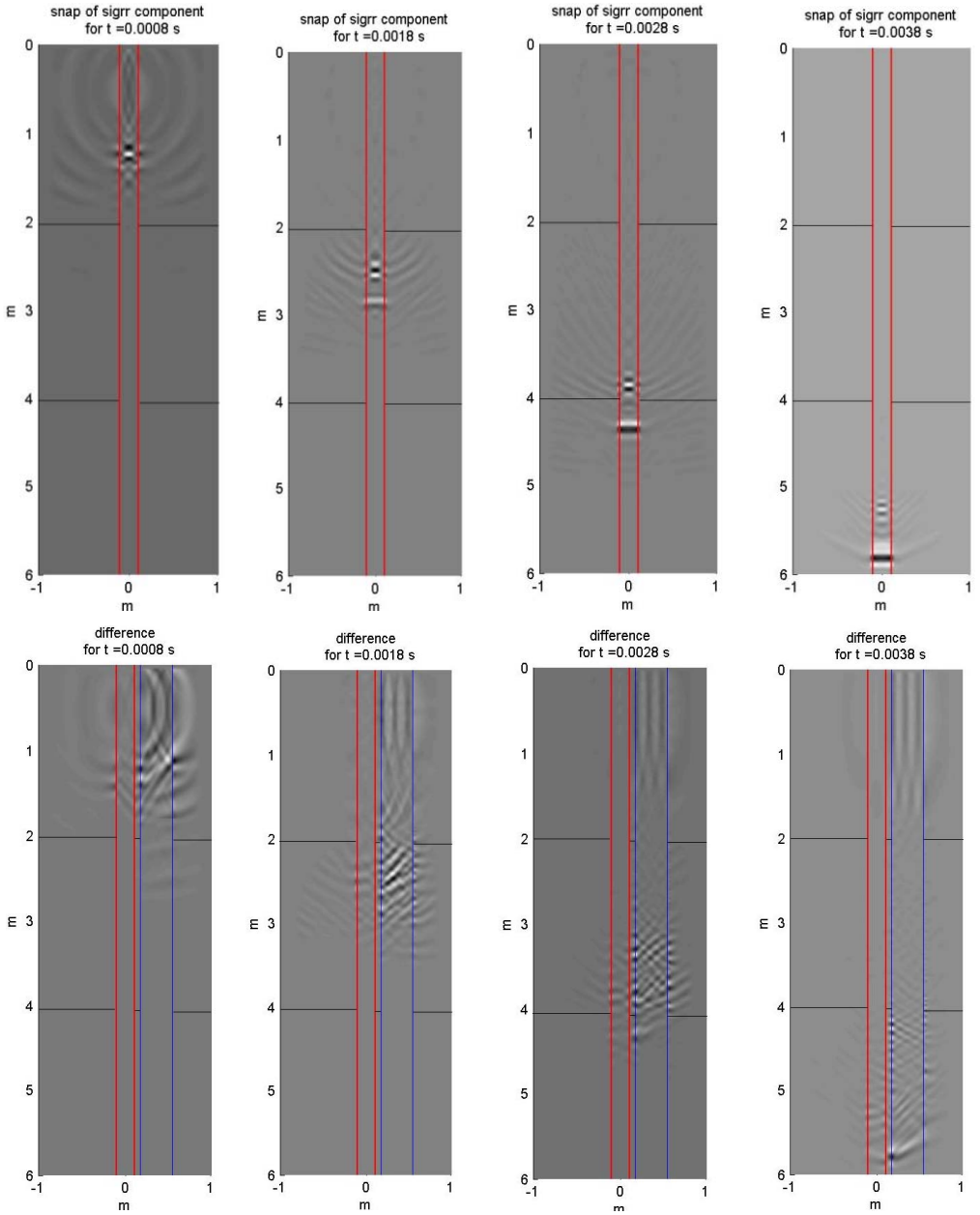

Figure 4. Snapshots for σ_{rr} propagating through the plane $\phi = (0\pi)$. Left column-the model without crack; Right column-difference between the calculations for the model with and without vertical crack.

during its propagation within borehole and adjacent rocks with and without of vertical crack. There is a series of snapshots for components through the plane $\varphi = (0,\pi)$ for axial source position with dominant frequency of 10 kHz located in $z = 0.5$ m. Two vertical red lines are projections of interface between borehole and its completion with surrounding rocks, black horizontal lines indicate interfaces of the layers and blue lines follow the crack. The left column figures illustrate wave propagation for the model without of crack, while the right column figures represent the propagation of difference between the wave field with and without of crack.

5. Conclusion

The current version of developed software for simulation of wave propagation in 3D heterogeneous viscoelastic multiscale media opens possibility of careful study of a rather wide range of realistic problems connected with borehole-based geophysics. Of course, this version is not perfect and should be further developed in different directions. In particular, one of the most challenging problems is to perform full scale simulation for media with extremely different scales, especially with microstructure like caverns, pores and so on. In order to do that with reasonable computer cost, one should be able to refine

locally not spatial grid cells only, but time step used for computations as well. Another important axis of development is connected with necessity to provide an opportunity to perform simulation for more realistic mechanical models and above all media with anisotropy induced by fine layering, clusters of microcracks and stresses around a well.

6. Acknowledgements

This work was supported by the Russian Foundation for Basic Research (projects no. 11-05-00947, 13-05-00076 and 13-05-12051).

REFERENCES

[1] J. O. Blanch, J. O. A. Robertsson and W. W. Symes, "Modeling of a Constant Q: Methodology and Algorithm for an Efficient and Optimally Inexpensive Viscoelastic Technique," *Geophysics*, Vol. 60, No. 1, 2005, pp. 176-184.

[2] R. M. Christensen, "Theory of Viscoelasticity—An Introduction," Academic Press, Waltham, 1982.

[3] S. Hestholm, *et al.*, "Quick and Accurate Q Parameterization in Viscoelastic Wave Modeling," *Geophysics*, Vol. 71, No. 5, 2006, pp. T147-T150.

[4] V. I. Kostin, D. V. Pissarenko, G. V. Reshetova and V. A. Tcheverda, "Numerical Simulation of 3D Acoustic Logging," *Lecture Notes in Computer Sciences*, Vol. 4699, 2007, pp. 1045-1054. http://dx.doi.org/10.1007/978-3-540-75755-9_122

[5] F. J. McDonal, F. A. Angona, R. L. Mills, R. L. Sengbush, R. G. van Nostrand and J. E. White, "Attenuation of Shear and Compressional Waves in Pierre Shale," *Geophysics*, Vol. 23, No. 3, 1958, pp. 421-439. http://dx.doi.org/10.1190/1.1438489

[6] S. A. Siddiqui, "Dispersion Analysis of Seismic Data," M.S. Thesis, University of Tulsa, Tulsa, 1971.

[7] P.C. Wuenschel, "Dispersive Body Waves—An Experimental Study," *Geophysics*, Vol. 30, No. 4, 1965, pp. 539-551. http://dx.doi.org/10.1190/1.1439620

